Chemical Aspects of Acylfulvene Bioactivation to a Cytotoxic Reactive Intermediate

A THESIS
SUBMITTED TO THE FACULTY OF THE GRADUATE SCHOOL
OF THE UNIVERSITY OF MINNESOTA
BY

Kathryn Elizabeth Pietsch

IN PARTIAL FULFILLMENT OF THE REQUIREMENTS
FOR THE DEGREE OF
MASTER OF SCIENCE

Professor Shana J. Sturla, Ph.D.

December 2009

ACKNOWLEDGMENTS

I would first and foremost, like to thank my advisor, Dr. Shana Sturla, for her continual guidance and support throughout my graduate studies thus far. I admire her thoughtful approach to scientific problems and aim to adapt a similar sense of creativity for my future studies and career. In addition to acting as an advisor who encourages my personal development as a scientist, she is also a friend who is truly concerned with my well-being, and I am excited to continue working with her at ETH in Zurich, Switzerland where I will carry out my doctoral studies.

Dr. Jiachang Gong and Jim Neels, former members of the Sturla research group, were responsible for conducting experiments in the initial stages of this project. I appreciate their prompt explanations and clarifications to any questions that arose throughout this work, as I never had the privilege to interact with them while they were active members of the lab. Dr. Xiang Yu also continues to serve as an expert who is only an email away. In addition to providing timely results as a collaborator, he has been more than willing to answer any questions and provide detailed explanations regarding work both related and unrelated to this project. I look forward to continuing to collaborate with him in future studies.

I would like to thank members of the Sturla research group for their feedback and support, especially Dr. Xiaodan "Kathy" Liu, Hailey Gahlon, and Dr. Marina Tanasova. Also, Dr. Sarah Kliegman, a former roommate and new friend, for helpful discussions and her KaleidaGraph expertise.

Drs. Lisa Peterson and Edgar Arriaga served as committee members for my defense. I appreciate their feedback and insight, as their varied backgrounds have provided unique points of view in regards to this project and its future.

Dr. Pete Villalta has been most helpful with all? experiments that have been carried out at the Analytical Biochemistry Facility at the Masonic Cancer Center (funding from the National Cancer Institute (NCI)). I look forward to working with him more closely in the near future as we get our new instruments up and running at ETH.

The NMR experiments carried out at the Structural Biology NMR Facility (funding from NSF BIR-961477, University of Minnesota Medical School, Minnesota Medical Foundation) would not have been possible without Dr. Beverly Ostrowski. Even though time was limited and the NMR facility was understaffed, Bev went above and beyond to find instrument time, set up experiments, create figures, and share her extensive knowledge with me. Her efforts are greatly appreciated.

This project would have required copious amounts of synthetic work had it not been for a generous gift of illudin S from MGI Pharma, Inc. The time saved in being able to prepare my starting material in one step is priceless.

Lastly, nothing is possible without money. I would like to acknowledge the University of Minnesota Graduate School and the NCI for financial support.

ABSTRACT

Understanding molecular mechanisms of cytotoxicity is vital to the development of more effective chemotherapies. Acylfulvenes (AFs) are a class of semisynthetic analogues of the natural product illudin S. Minor structural changes between the parent compound and AFs have resulted in a more favorable selectivity profile in preclinical chemotherapy assays. AF cytotoxicity involves alkylation of biological targets, including DNA and cellular proteins. While AFs are capable of direct alkylation, reductive bioactivation to an electrophilic intermediate is correlated with enhanced cytotoxicity. Alkenal/one oxidoreductase (AOR) is a cytosolic enzyme implicated in activating AF in cells that are sensitive to the drug. This study aims to elucidate chemical aspects of acylfulvene activation mechanisms. We compared enzymatic versus chemical activation pathways for AF involving NADPH-dependent AOR or sodium borohydride, respectively. These two processes result in isomeric reactive intermediates. Despite structural differences, these isomers appear to have similar biological activity and give rise to similar patterns of DNA modification. Cell-based studies, utilizing human embryonic kidney cells transiently transfected with an AOR-overexpressing vector, were conducted to test the hypothesis that a chemically activated AF does not require further bioactivation to be cytotoxic. The reactivity of this activated compound was further assessed by measuring its half-life in the presence of acid. On the basis of this study, we anticipate that the chemically activated form of AF will serve as a useful tool for evaluating protein and nucleic acid interactions, and to gain a further understanding of their contributions to cytotoxicity, independent of bioactivation.

TABLE OF CONTENTS

LIST OF FIGURES

INTRODUCTION

Bioactivation is the metabolic transformation of unreactive compounds to biologically reactive intermediates capable of interacting with or modifying biological targets. Xenobiotics that are converted to alkylating agents after enzymatic reduction are considered bioreductive alkylating agents.[1-2] One related drug design strategy exploits the structural features of prodrugs that are susceptible to bioreductive activation. Tumor tissue capable of bioactivating the prodrug will be susceptible to damage resulting from the activated drug's electrophilicity, and tissue that is unable to reduce the prodrug will not be damaged.[3-4]

DNA-alkylating agents are amongst the most widely used and effective forms of cancer chemotherapy. Resulting DNA damage can lead to a variety of outcomes, ranging from successful repair to cell cycle arrest, apoptosis, and/or mutagenesis.[5] Despite recent advances in the efficacy of targeted therapies, alkylating agents still make valuable contributions in the cancer treatment arena.

Due to the continued need for more selective chemotherapies, identifying characteristics that differentiate tumor cells from normal cells is critical. One such factor is the reductive microenvironment of hypoxic tumors. Angiogenesis generally lags behind rapidly dividing tumor cells, resulting in solid tumors that lack complete microvascularization. Consequently, tumors become hypoxic and there are no avenues for drug delivery to malignant cells. In addition to the reductive environment, tumor cells often overexpress reductive enzymes.[4] Understanding the reductive potential of tumor cells and how they transform drugs can lead to improved design of selective therapies that rely on a certain enzyme or microenvironment for activation.

For developing and better understanding modes of action of bioreductively activated cancer chemotherapy drugs, the ability to synthesize a corresponding reactive intermediate would facilitate the study of potential biomacromolecule adducts, specifically, their structures and contributions to cytotoxicity. If the reactive intermediate can be synthesized, it can be useful in understanding mechanisms which will lead to improved drug design.

Acylfulvenes (AFs) are semi-synthetic derivatives of the natural products illudin M and S (Figure 1), metabolites from *Omphalotus illudens*.[6] The illudins are potent tumor cell toxins but exhibit low therapeutic indices.[7] AFs have improved therapeutic indices compared to their parent illudins, which is likely the result of many contributing factors. One AF analogue, (hydroxymethyl)acylfulvene (HMAF), started in clinical trials at the end of 1995.[8]

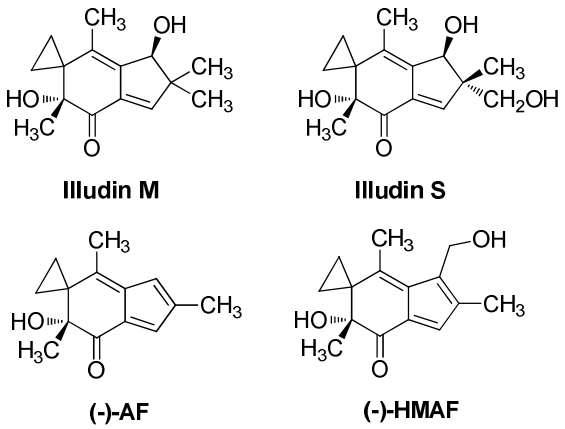

Figure 1. Natural product illudins and semi-synthetic analogues, AF and HMAF.

It is well accepted that the cytotoxicity of AFs can be attributed to alkylation of important biomolecules such as DNA and proteins. A preliminary mechanism of action, involving conjugate addition to the α,β-unsaturated ketone and nucleophilic opening of the cyclopropyl ring, was proposed by T. C. McMorris et al.[9] and has been refined over the past two decades. Furthermore, early cytosolic metabolism studies by McMorris et al. suggested that AFs undergo enzymatic activation requiring NADPH as cofactor. It was hypothesized that hydride delivery from NADPH to the α,β-unsaturated ketone gives rise to an electrophilic intermediate capable of alkylating cellular nucleophiles (Figure 2).[6]

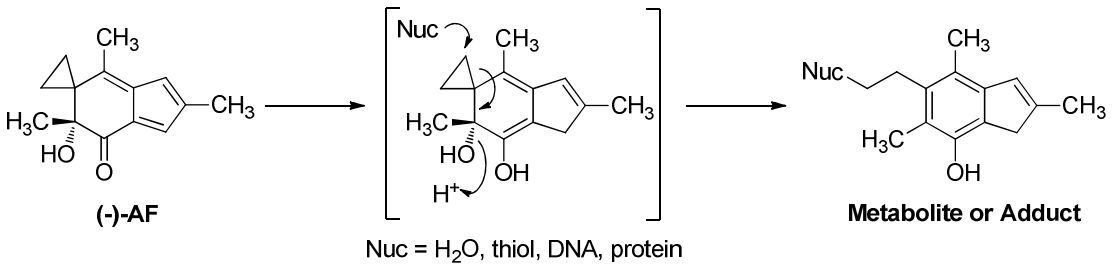

Figure 2. Mechanism of metabolite or adduct formation from AF's putative reactive intermediate.

AF is capable of forming two different types of DNA adducts that result from different reaction pathways. As shown in Figure 3, one type of adduct arises from direct Michael-type addition of nucleobase-centered nucleophiles to the α,β-unsaturated ketone of AF, and the second type of adduct is the product of enzymatic reduction followed by cyclopropyl ring opening.

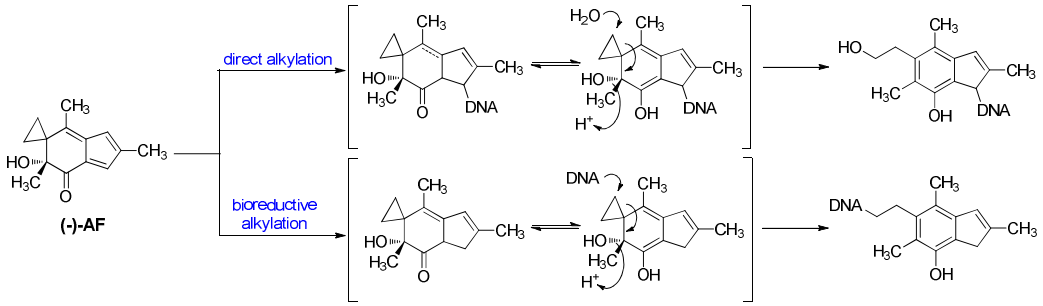

Figure 3. Proposed pathways for the formation of two types of AF-DNA adducts.

We have previously reported that the quantity of the direct addition adenine adduct, resulting from AF reacting with ctDNA in the absence of AOR, is much lower (0.1%) than that resulting from nucleophilic attack of AF's bioactivated intermediate by ctDNA deoxyadenosine.[10] However, based on precedence regarding O^6-methyl dG adducts, quantity of adducts does not necessarily overshadow the adduct type. In the case of O^6-methyl dG, this low abundant adduct can be extremely detrimental if not repaired in a timely manner. One can then imagine that a chemical probe that mimics the bioactivated intermediate of AF would enable studies of adducts that arise from this intermediate and how they contribute to AF's overall cytotoxicity.

AFs have been identified as substrates for the NADPH-dependent enzyme alkenal/one oxidoreductase (AOR).[11-12] AOR is an inducible, cytosolic enzyme that catalyzes the reduction of the carbon-carbon double bond of α,β-unsaturated ketones and aldehydes.[13] In normal cells, this antioxidative enzyme detoxifies electrophilic substrates, like lipid peroxidation products, which prevents biological adduct formation.[13] However, for AF, a positive correlation exists between AOR levels and cell

sensitivities;[11-12, 14] cells with high levels of AOR are more capable of quickly activating AFs to a reactive species that induces toxicity.

For illudin M, enzymatic reduction by AOR occurs from the pro-*R* face of NADPH, thereby installing the *R*-configuration at C8, as illustrated in Figure 4.[15] In the case of AF, however, neither the stereochemistry nor regiochemistry of the biochemical transformation has been investigated. Considering the important contributions of AOR-mediated activation, and the toxicity of the reduced form of AF, in dictating the activity and selectivity of the drug, it is of interest to characterize chemical and biochemical aspects of the mechanism of reduction and nature of the activated intermediate. To this end, a reduced biologically reactive AF derivative is expected to be an important biological probe. We posited that our ability to generate and purify a chemically activated intermediate would allow us to identify and examine DNA and protein adducts that contribute to AF's cytotoxicity. In addition, we would be able to deliniate chemical pathways contributing to AF toxicity independent of enzymatic activity. Studies presented here provide access to a new AF-derived mechanistic probe of toxicity and detailed chemical and biochemical mechanistic information regarding reductive processes that activate the AF framework to an electrophilic species.

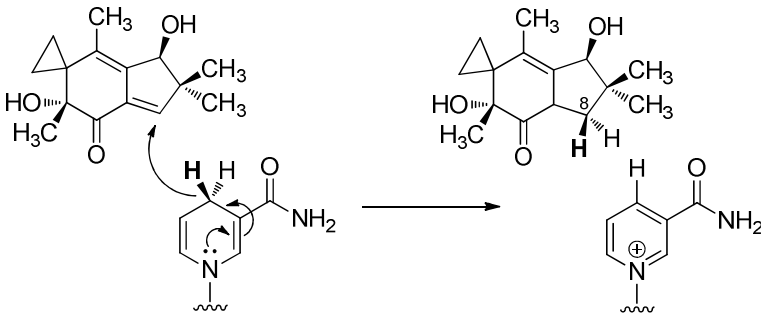

Figure 4. Catalytic transfer of NADPH's pro-R hydride to the α,β-unsaturated ketone of illudin M.

RESULTS

Chemical activation of AF

To define the regiochemistry associated with AOR-mediated AF bioactivation, AF was subjected to enzymatic reduction by AOR in the presence of either NADPH or d_2-NADPD. The major metabolite M1, which results from reduction followed by hydrolytic cyclopropane cleavage and aromatization (Figure 5), was isolated.

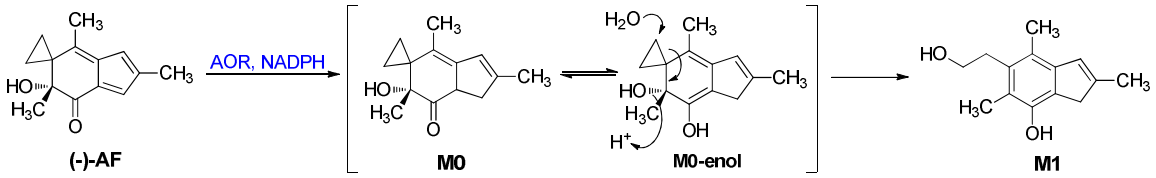

Figure 5. Mechansim for metabolite M1 formation following enzymatic bioactivation by AOR in the presence of NADPH.

Mass analysis of the resulting M1 indicated that the product mass was *m/z* 220[16]. Thus, these data were consistent with bioreduction occuring via a 1,4-pathway, i.e. conjugate addition to the α,β-unsaturated ketone at C8 (Figure 6a), or a 1,6-pathway with addition occurring to the extended conjugated system at C6 (Figure 6b). For a 1,8-reduction mechanism, one would anticipate to detect *m/z* 219, suggesting that the metabolite is deuterated at the C4 position followed by deuterium loss during the conversion to M1 (Figure 6c).

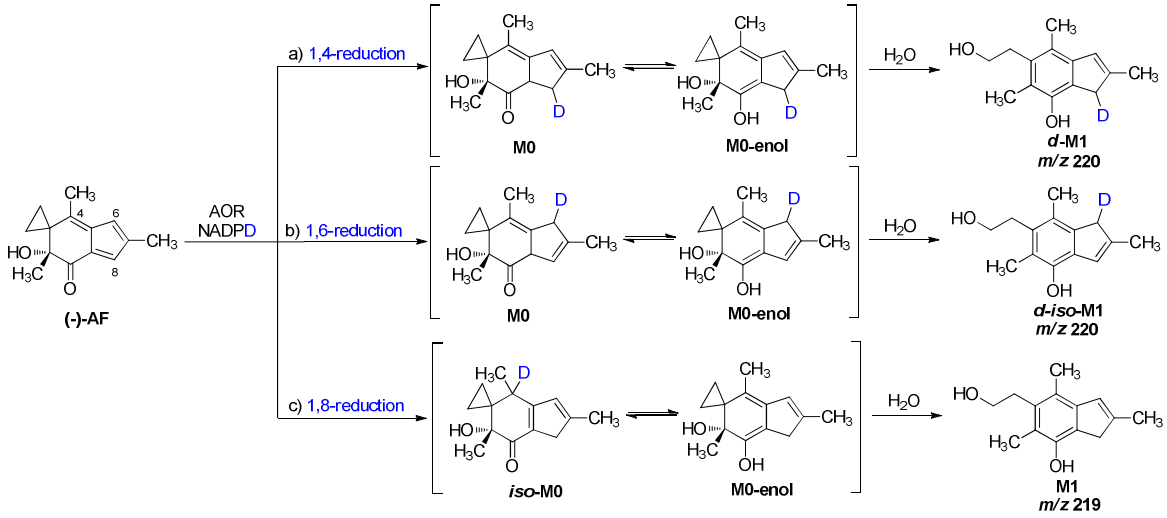

Figure 6. Possible sites of enzymatic reduction of AF by AOR in the presence of NADPD, followed by metabolite formation. a) 1,4-reduction pathway resulting in metabolite *m/z* 220. b) 1,6-reduction pathway resulting in metabolite *m/z* 220. c) 1,8-reduction pathway resulting in metabolite *m/z* 219.

In preliminary studies in our lab, James Neels found reaction conditions, involving sodium borohydride in pyridine, that mediate the chemical reduction of AF.[17] The structure of the resulting chemical species was assigned by Neels as *iso*-M0 on the basis of NMR and MS data. In particular, the presence in the ^{1}H NMR (Figure 8, panel A) of a doublet at 0.95 ppm associated with C4 is diagnostic, making M0 an inconsistent structural representation because in M0, two of the methyl groups would be appended to sp^2 hybridized carbons and the third would be part of a quaternary center, i.e. all singlets.

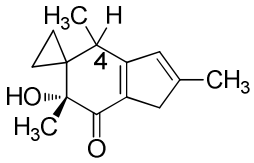

Figure 7. Structure of *iso*-M0.

Data from NOESY experiments provided further evidence that the pattern of double bonds in the cyclopentadiene ring are as depicted in Figure 7 (*iso*-M0). In addition, the molecular weight of *iso*-M0, *m/z* 218 is consistent with the observed *m/z* 241 [M + Na^+]. *Iso*-M0, therefore, results from hydride addition to C4, i.e. the exocyclic fulvene double bond of AF, and is an isomer of M0.

It was necessary to prepare pure samples of *iso*-M0 in order to test its biological properties. Initial attempts to purify *iso*-M0 by column chromatography on silica with an isocratic mobile phase (10% ethyl acetate, 90% hexanes) were unsatisfactory due to

contaminated fractions of *iso*-M0 eluting from the column. Thus, a mobile phase gradient (100% hexanes → 5% hexanes → 10% hexanes) was employed to purify *iso*-M0 from polar and non-polar impurities, including pyridine (30% yield). In addition, due to lack of UV activity in dilute fractions, phosphomolybdic acid staining was appropriate for visualization of *iso*-M0 when monitoring purification progress with TLC.

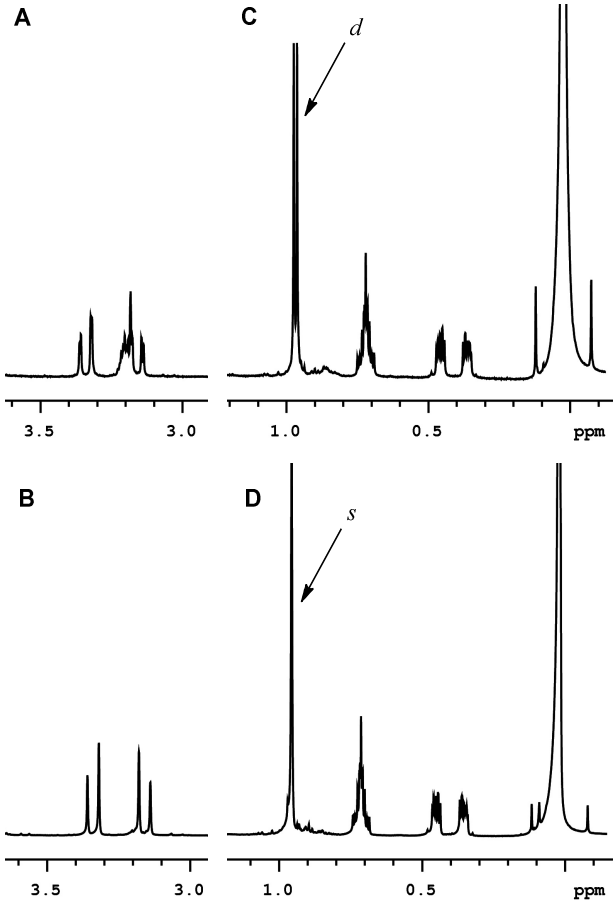

Figure 8. NMR spectra for *iso*-M0 (panels A, C) and *d-iso*-M0 (panels B, D). A) $q + q_{AB}$ signal associated with C4 and C8 protons in *iso*-M0. B) q_{AB} signal associated with C8 protons in *d-iso*-M0. C) *d* resulting from C4-CH_3 coupling to C4 proton of *iso*-M0. D) *s* associated with C4-CH_3 in *d-iso*-M0.

The cytotoxicity of iso-M0 was assayed in HEK-293T cells transiently transfected with a blank or AOR-overexpressing vector.[13] These experiments were carried out in collaboration with Dr. Xiang Yu at the National Institutes of Health. These engineered cells were utilized in previous studies[11-12] aiming to examine AOR's role in cells that are sensitive to AFs. Briefly, cells engineered with an AOR-overexpressing vector are sensitive to AF, as they are more capable of activating AFs than cells with lower levels of AOR, which are those that are transiently transfected with a blank vector. If *iso*-M0 is an already activated species, it should not require further activation to be cytotoxic. Thus, we hypothesize that its IC_{50} values should be similar between AOR-transfected and control cells, despite differences in AOR expression.

The regiochemistry of $NaBH_4$-mediated AF reduction was confirmed by carrying out the reaction with sodium borodeuteride. The ^1H NMR doublet at δ 0.95 ppm, associated with the C4 proton of *iso*-M0 (Figure 8, panel C), collapses to a singlet in the case of the deuterated analogue, *d-iso*-M0 (Figure 8, panel D). The $q + q_{AB}$ signal at δ 3.13–3.36 ppm, which arises from protons at C4 and C8 in *iso*-M0 (Figure 8, panel A), is a q_{AB} in *d-iso*-M0 (Figure 8, panel B). These data are consistent with the presence of a deuterium atom at the 4-position and confirm that the hydride is delivered to the C4 position.

In the course of these studies, I observed that the efficiency of the $NaBH_4$-mediated reduction is very sensitive to the activity of the reducing reagent, and therefore conditions had to be optimized to avoid product degradation. In the case of a fresh bottle of $NaBH_4$ or $NaBD_4$, a solution of AF in dry pyridine is added to a 0 ^oC $NaBH_4$ or $NaBD_4$ solution in dry pyridine. The mixture is allowed to stir at room temperature until a complete color change from yellow to pale brown is observed (usually less than 20 minutes). If a second color change occurs, usually to dark brown, the desired product has been degraded with no recognizable ^1H NMR signal. Optimized gradient chromatography, as described above, was also applied to *d-iso*-M0 purification.

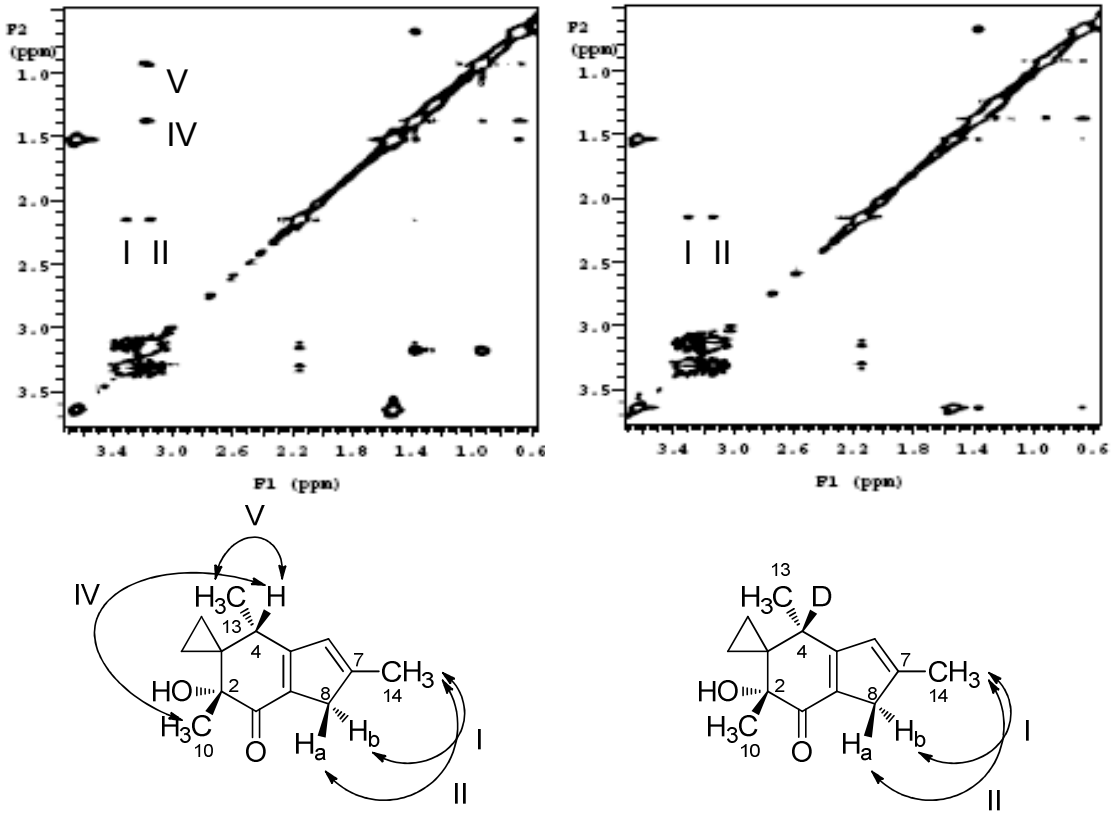

Figure 9. NOE interactions in *iso*-M0 (left) and *d-iso*-M0 (right).

The relative and absolute stereochemistry at C4 was assigned on the basis of correlations in the 2D-NOESY spectra of *iso*-M0 and *d-iso*-M0. Relevant NOESY cross-peaks are labeled in Figure 9. NOE interactions I and II arise from interactions between both protons at C8, which are on either side of the plane of the cyclopentadiene, and are present in *iso*-M0 and *d-iso*-M0 spectra. NOE interaction V involves H4 and adjacent C13-CH_3, which is expected as both moieties are appended to the same carbon. The alignment of NOE V and IV suggests that H4 also interacts with C10-CH_3. These data, together with the lack of NOE interaction between C13-CH_3 and C10-CH_3, suggests that the new proton H-4 is on the same face of the molecule as C10-CH_3. Analogous cross-peaks are not present in the NOESY spectra obtained for *d-iso*-M0; the lack of NOE IV and V further suggests that the chemical reduction produces the *S*-stereochemistry pictured in Figure 9.

Reactivity of *iso*-M0

To evaluate whether *iso*-M0 is a viable chemical precursor to M1, we tested its chemical reactivity at varying pH and in the presence of nucleosides and DNA. M0-enol is a common tautomer of both M0 and *iso*-M0, it was anticipated that iso-M0 would give rise to the same major metabolite as bioactivated AF, i.e. M1. Such a conversion would involve hydrolytic cyclopropyl ring opening as depicted in Figure 10. In preliminary

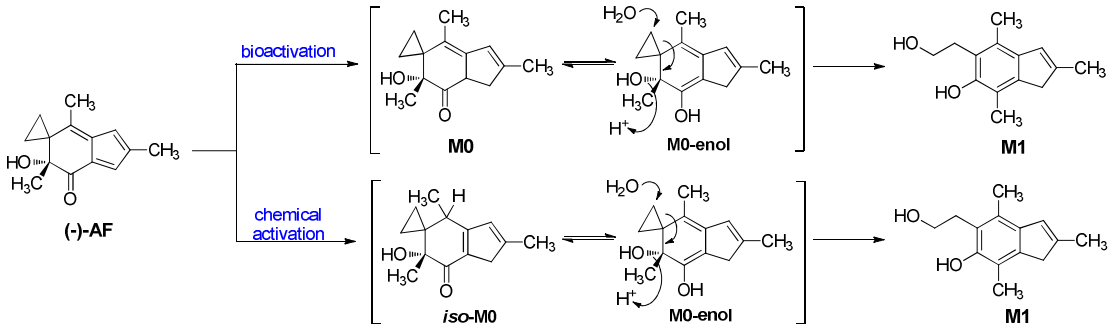

Figure 10. Comparison of pathways pertaining to the enzymatic and chemical reduction of AF. M0-enol is postulated as a common intermediate for both pathways.

studies carried out by Jiachang Gong, it was observed that *iso*-M0 in sulfuric acid/THF yields M1 (Figure 11).[18] *d-iso*-M0 is also converted to M1 under similar acidic conditions (Figure 11).

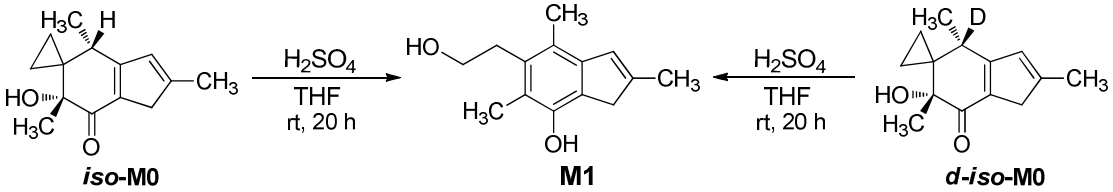

Figure 11. Conversion of *iso*-M0 and *d*-iso-M0 to M1.

The stability of *iso*-M0 was assessed by measuring its half-life under acidic, neutral, and basic conditions. This study was conducted by time-course NMR analysis of standardized *iso*-M0 solutions. NMR experiments were carried out in THF-d_8 and dimethyl sulfone was used as an internal standard.[19] Reactions were initiated by adding 200 µL 10% H_2SO_4, 10% NaOD, or D_2O at 25 ^oC to a THF solution of *iso*-M0 (3

mg/mL). ^{1}H NMR spectra were acquired every 10 minutes for 12 hours. Preliminary results for experiments described above were as follows: under acidic conditions (THF-d_8:10% aq. H_2SO_4= 2.2, pH 1) there was no detectable spectral changes after one day, but completely converted to M1 in less than 30 days. As anticipated, *iso*-M0 rapidly reacted upon addition of NaOD (THF-d_8:base = 2.2, pH 11), but surprisingly, M1 never was observed. Thirty days after adding D_2O (THF-d_8:D_2O = 2.2, pH 7) to the standardized *iso*-M0 solution, no conversion to M1 had occurred.

A subsequent study focused on measuring the rate of the acid-mediated conversion of *iso*-M0 to M1. H_2SO_4 was added to a solution of *iso*-M0 in THF-d_8 (11.5 mg/mL), resulting in a 1:2 ratio of THF-d_8:4 N aq. H_2SO_4 (pH 1). The chemical transformation was monitored by acquiring an NMR spectrum every 5 minutes for 12 hours. Chemical shifts were referenced to THF-d_8 at δ 1.72 and 3.58 ppm, and peak area integrals were standardized to that of the internal standard, dimethyl sulfone (δ 3.00, s, 6H). A sample of arrays from a representative experiment (5.8 mg/mL *iso*-M0 in THF-d_8, THF-d_8:H_2SO_4 ratio of 1:2 (pH 1)) is displayed in Figure 12A.

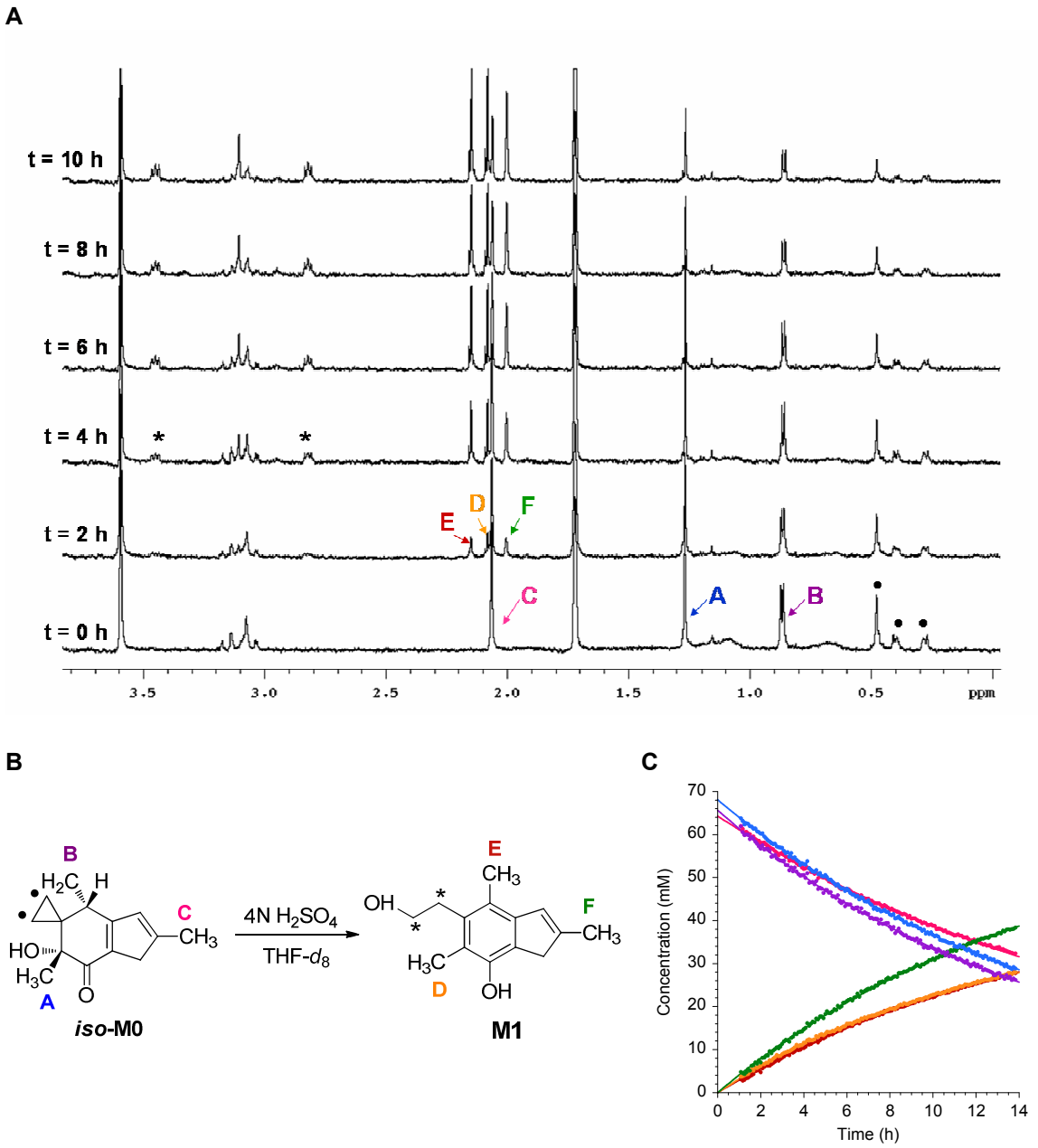

Figure 12. Acid-mediated conversion of *iso*-M0 to M1, monitored via NMR. A) Array of NMR spectra tracking the conversion from *iso*-M0 to M1 upon addition of acid. Peaks denoted with • and * represent the closed and opened cyclopropane ring, respectively; B) Key for methyl peaks assignments in *iso*-M0 and M1; C) Plot of change in concentration versus time. Color-coded data points and curve fits follow key in part B.

At t = 0 h, only peaks associated with the starting material, *iso*-M0, are present in the spectra and decreases in peak size are seen at the next timepoint. Twenty minutes

into the reaction, signals associated with the methyls in M1 start to emerge from the baseline. It seems that cyclopropyl ring opening does not start to occur until t = 1.5 h with the appearance of triplets at δ 2.8 and 3.4 ppm, but this is not the case. Since peaks integrating to fewer protons have smaller areas, their initial appearance may not be differentiated from the baseline, thereby seeming to appear at later timepoints with slower rates. With this in mind, we decided to calculate the rate constant, *k*, using only the well-distinguished methyl groups highlighted in Figure 12B. Figure 12C shows the decay and growth of peaks associated with those methyls with respect to time. Using KaleidaGraph (version 4.0)**,** the data was fit with exponential curves and the average first-order rate constant, based on the decay of methyls A-C, was 1.7 ± 0.2 x 10^{-5} s^{-1}, corresponding to a $t_{1/2}$ of 11.6 h.

Reactions of *iso*-M0 with nucleosides and ctDNA

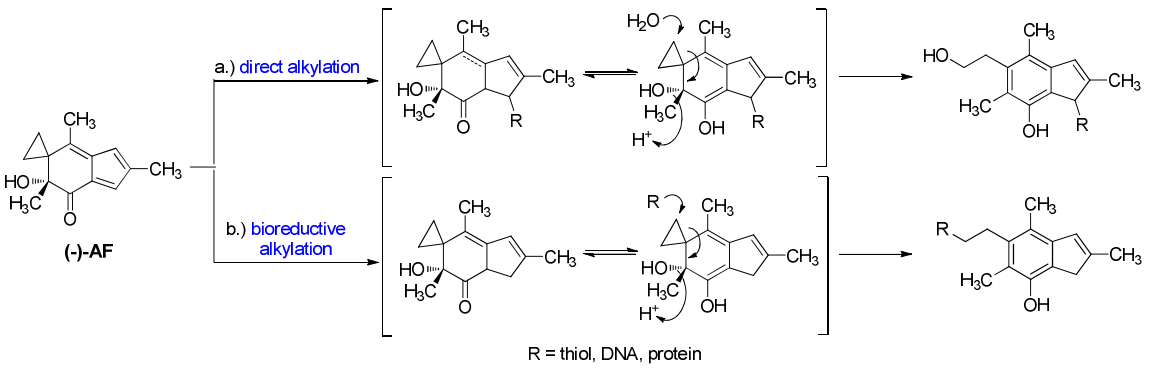

Figure 13. Contributing pathways for AF-mediated metabolism.

For *iso*-M0 to be a viable mechanistic probe for studying AF-mediated alkylation of cellular targets resulting from the bioactivation-mediated reactivity manifold (Figure 13b), but independent of enzymatic reduction, and without competitive direct-alkylation reactions (Figure 13a), its molecular reactivity should mirror that of enzymatically reduced AF. DNA adducts arising from alkylation by bioactivated AF of a variety of deoxyribose nucleic acids have been previously reported by us.[10] In the presence of AOR and NADPH or rat liver cytosol, AF has been shown to preferentially alkylate purine

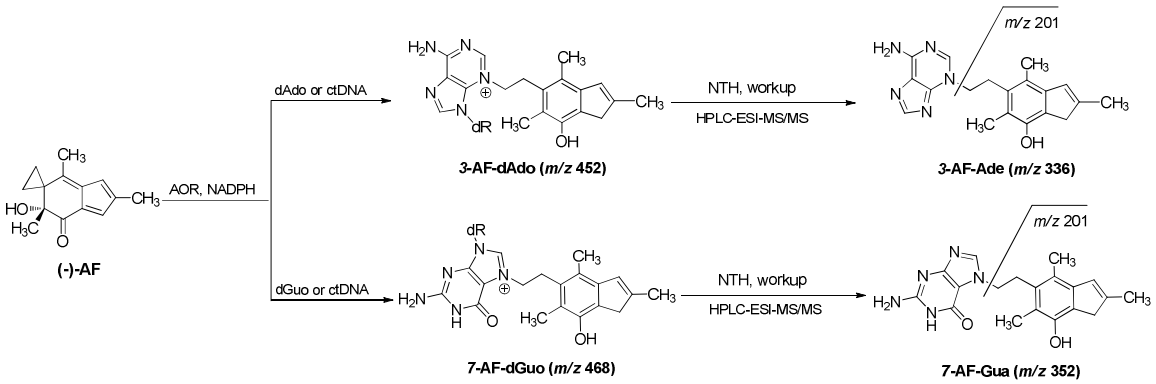

Figure 14. Reaction of bioactivated AF with purine bases. The DNA adducts and resulting fragments are identified via known *m/z* values.

bases as single nucleosides and in calf thymus DNA (ctDNA), and these known adducts have been detected in cells. The major DNA adducts, 3-AF-deoxyadenosine (3-AF-dAdo) and 7-AF-deoxyguanosine (7-AF-dGuo), formed by AF in the presence of AOR and NADPH, are thermally unstable and depurinate during neutral thermal hydrolysis (Figure 14).[10] Thus, in the present study, we aimed to determine whether *iso*-M0 alkylates DNA in a similar manner as bioactivated AF.

The reaction of *iso*-M0 with individual nucleosides was compared with the reaction products from bioactivated AF with isolated nucleosides. *Iso*-M0 was allowed to react with dAdo, dGuo, or ctDNA in aqueous solution (pH 7) at 37 ^{o}C for at least 24 hours. Samples were heated at 90 ^{o}C for 60 min to induce neutral thermal hydrolysis. Sample workup entailed water removal via rotary evaporation, solid phase extraction with methanol, filtration, and methanol removal via rotary evaporation. Samples were reconstituted in methanol and assayed for adduct formation by comparison with authentic standards of 3-AF-Ade and 7-AF-Gua.[10] Reactions with dAdo or dGuo resulted in peaks with *m/z* 336 or 352, respectively, which fragment to *m/z* 201, representative of AF's characteristic indene moiety (Figure 14). In addition, fragments corresponding to the base portion of the adduct, *m/z* 136 for Ade and *m/z* 152 for Gua, were also detected and peak shapes matching those of the *m/z* 201 fragment provide further evidence for the AF-DNA adducts. As seen in Figure 15A, peaks resulting from the reaction of AF in the presence of AOR and NADPH and dGuo fragments to *m/z* 201 (panel i) and *m/z* 152

(panel ii) and the larger peaks (for both fragments) elute at a retention time similar to that of the of the 7-AF-Gua standard. It is possible that the earlier eluting peaks may arise from the fragmentation of the 3-AF-Gua adducts, as it is known that the 3-AF-Gua adduct has a shorter retention time than that of 7-AF-Gua.[10] A similar peak, arising from the reaction of *iso*-M0 with dGuo, albeit smaller, also elutes at the same time as the *m/z* 201 fragment of the 3-AF-Ade standard (~17 min), but is not the major product peak of the reaction. The major peak of this reaction mixture doesn't correlate to any peaks resulting from the reaction of bioactivated AF with dGuo, which suggests that chemically activated AF may be capable of yielding another depurinating adduct with *m/z* 352.

Chromatogram traces associated with the analysis of reactions with dAdo are in Figure 15C-D. The retention times of the major peaks resulting from the reactions of bioactivated AF and *iso*-M0 with dAdo (Figure 15C, 15D, respectively) match that of the Ade standard, and the corresponding mass spectra show that fragmentation of 3-AF-Ade results in *m/z* 201 and 136 (*m/z* 136 not labeled in Figure 15D).

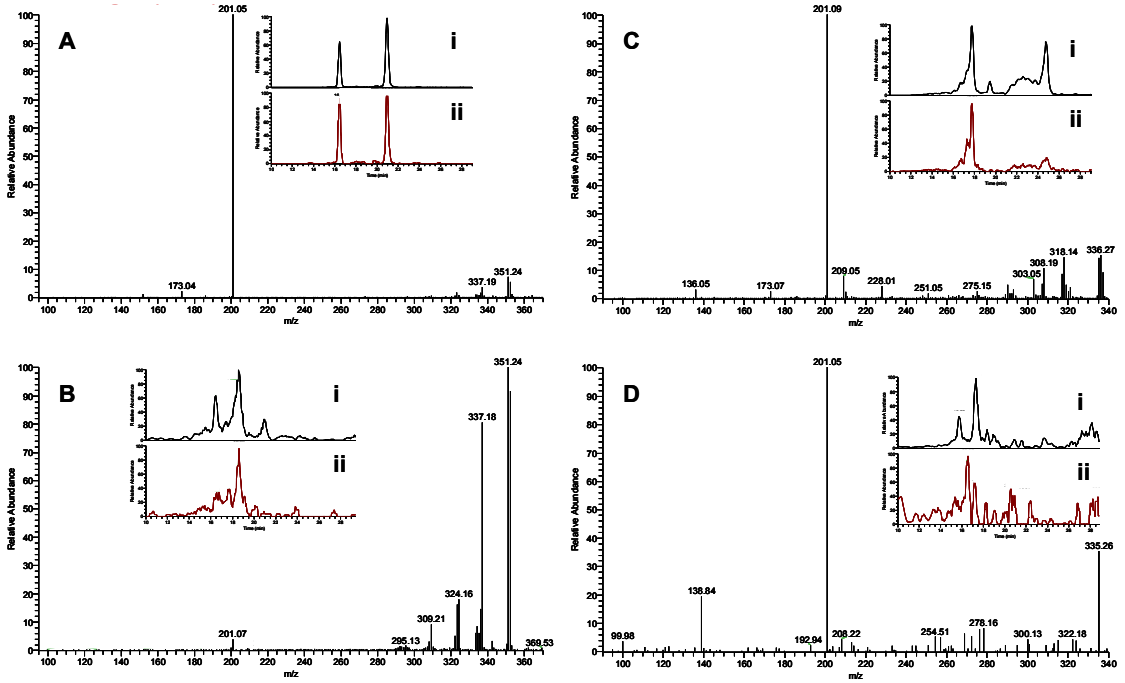

Figure 15. HPLC-MS^2 analysis of monomeric nucleoside reactions with *iso*-M0 and bioactivated AF. **A)** MS^2 *m/z* 352 → 201 mass spectra for the reaction of bioactivated AF with dGuo. Extracted ion chromatographs for MS^2 *m/z* 352 → 201 (i) and MS^2 *m/z* 352 → 152 (ii). **B)** MS^2 *m/z* 352 → 201 mass spectra for the reaction of chemically activated AF (*iso*-M0) with dGuo. Extracted ion chromatographs for MS^2 *m/z* 352 → 201 (i) and MS^2 *m/z* 352 → 152 (ii). **C)** MS^2 *m/z* 336 → 201 mass spectra for the reaction of bioactivated AF with dAdo. Extracted ion chromatographs for MS^2 *m/z* 336 → 201 (i) and MS^2 *m/z* 336 → 136 (ii). **D)** MS^2 *m/z* 336 → 201 mass spectra for the reaction of chemically activated AF (*iso*-M0) with dAdo. Extracted ion chromatographs for MS^2 *m/z* 336 → 201 (i) and MS^2 *m/z* 336 → 136 (ii).

The reactivity of bioactivated AF or *iso*-M0 with ctDNA was examined in a manner similar to studies with individual nucleosides described above. It is evident that the reaction of ctDNA with bioactivated AF yields two products with *m/z* 352, with the latter and more prevalent peak corresponding to 7-AF-Gua fragments (16A, panels i and ii). In the case of the guanine adducts, the larger peak resulting from the reaction of ctDNA with *iso*-M0 has a fragment *m/z* 201, but chromatogram associated with fragment *m/z* 152, compared to *m/z* 201, is extremely minor. Therefore, it is possible that *iso*-M0 forms the 7-AF-Gua adduct in the presence of ctDNA, but at low levels. Formation of 3-AF-Ade in the reaction of *iso*-M0 with ctDNA is confirmed, as the resulting *m/z* 336 peak that fragments to *m/z* 201 and 136 and has a retention time of 17 min (Figure 16D), which

matches the retention times of both authentic 3-AF-Ade standard and the adduct resulting from the reaction of bioactivated AF with ctDNA (Figure 16C).

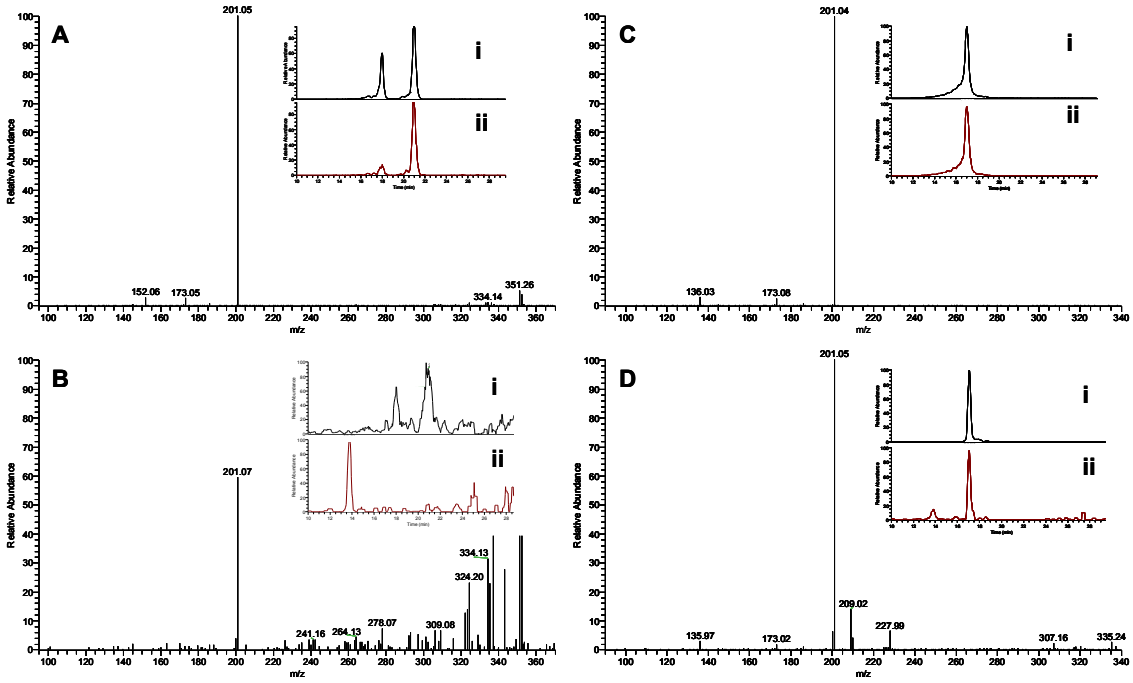

Figure 16. HPLC-MS^2 analysis of ctDNA reactions with *iso*-M0 and bioactivated AF**. A)** MS^2 *m/z* 352 → 201 mass spectra for the reaction of bioactivated AF with ctDNA. Extracted ion chromatographs for MS^2 *m/z* 352 → 201 (i) and MS^2 *m/z* 352 → 152 (ii). **B)** MS^2 *m/z* 352 → 201 mass spectra for the reaction of chemically activated AF (*iso*-M0) with ctDNA. Extracted ion chromatographs for MS^2 *m/z* 352 → 201 (i) and MS^2 *m/z* 352 → 152 (ii). **C)** MS^2 *m/z* 336 → 201 mass spectra for the reaction of bioactivated AF with ctDNA. Extracted ion chromatographs for MS^2 *m/z* 336 → 201 (i) and MS^2 *m/z* 336 → 136 (ii). **D)** MS^2 *m/z* 336 → 201 mass spectra for the reaction of chemically activated AF (*iso*-M0) with ctDNA. Extracted ion chromatographs for MS^2 *m/z* 336 → 201 (i) and MS^2 *m/z* 336 → 136 (ii).

DISCUSSION

AFs are a class of natural product derivatives that are cytotoxic to tumor cells, and it has been demonstrated that AFs undergo bioreductive activation to a putative electrophilic intermediate in a process relevant to its toxicity profiles. The posited enzyme contributing to catalyzing the reduction of AFs is AOR, a NADPH-dependent enzyme that serves to detoxify small electrophilic species within cells. In the case of AFs, AOR's antioxidative function activates these compounds to alkylating agents, and a positive correlation between AOR levels, AF-DNA adducts, and cell sensitivity has been confirmed.[10-11] Based on the importance of reductase-mediated activation, it is of interest to understand its mechanism and to obtain a chemically activated analogue that could be used to gain a better understanding of biological adduct formation and cytotoxicity independent of enzymatic bioactivation. This study details the chemoselectivity of AF bioreduction, the synthesis and purification of our chemically reduced form of AF (*iso*-M0), as well as the characterization of its stability and reactivity profile with DNA.

The regiochemistry of AF reduction catalyzed by AOR was evaluated by carrying out enzyme-mediated reductions with isolated enzyme and deuterium-labeled cofactor NADPH (d_2-NADPD). The resulting product M1 had a *m/z* 220, consistent with a 1,4- or 1,6-reduction. It has been demonstrated previously[13] that AOR catalyzes the reduction of α,β-unsaturated ketones or aldehydes via hydride addition to the β-carbon (i.e. 1,4-reduction). On the basis of the MS data obtained here and precedent, it is likely that the reduction occurs by an analogous mechanism, however a potential 1,6-pathway cannot be strictly excluded.

In contrast to the observation that AOR catalyzes hydride addition to C6 in the case of the 1,4-pathway, reduction of AF with the chemical hydride source $NaBH_4$ yields *iso*-M0, resulting from delivery of the hydride to C4. *Iso*-M0 is a different isomer compared to the proposed bioactivation product, and the regiochemistry of the reduction is consistent with literature precedent. Literature examples demonstrate that strong hydride reducing agents, like alkyllithium reagents[20] and lithium triethylborohydride[21] are generally required to reduce fulvenes, but here we demonstrate fulvene reduction with the

mild reducing agent $NaBH_4$. A dipolar resonance structure with an aromatic cyclopentadiene ring, suggested by McMorris et al.[6, 22] (Figure 17), is useful in rationalizing the observed regioselectivity of the chemical reduction. In addition, it is possible that the carbonyl may tune the reduction potential of the fulvene.

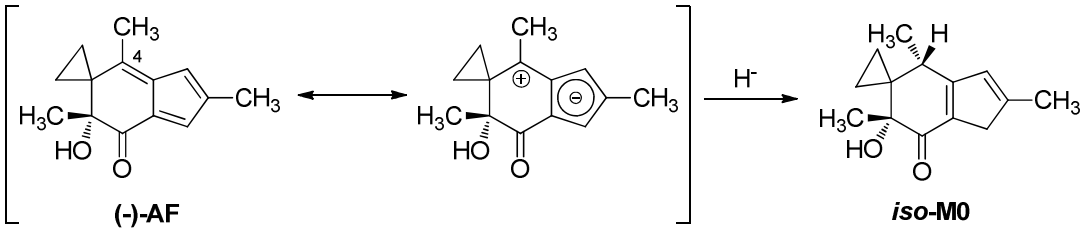

Figure 17. Reduction of AF's dipolar resonance structure to yield *iso*-M0.

Results described here regarding the reaction of $NaBH_4$ with AF demonstrate that this chemical reduction process is diastereoselective, leading to the exclusive formation of *S*-*iso*-M0, and resulting from hydride addition to the *si* face of the molecule. While it was not surprising that *iso*-M0 is produced as a single diastereomer, i.e. $NaBH_4$ is a stereoselective and chemoselective reducing agent,[23] the observed facial stereoselection occurred in the opposite manner of similar systems. Our initial hypothesis was that, in the $NaBH_4$-mediated reduction, the hydride would be delivered to the *re* face of AF, directed by chelation control with the C2-OH and avoiding unfavorable steric interactions with C2-CH_3. A potential explanation for the stereoselectivity of the observed chemical reduction involves the avoidance of unfavorable steric interactions in the product. Thus, if hydride delivery to C4 were directed by the hydroxyl group to the *re* face, the methyl groups at C2 and C4 would be *syn* in the product, resulting in

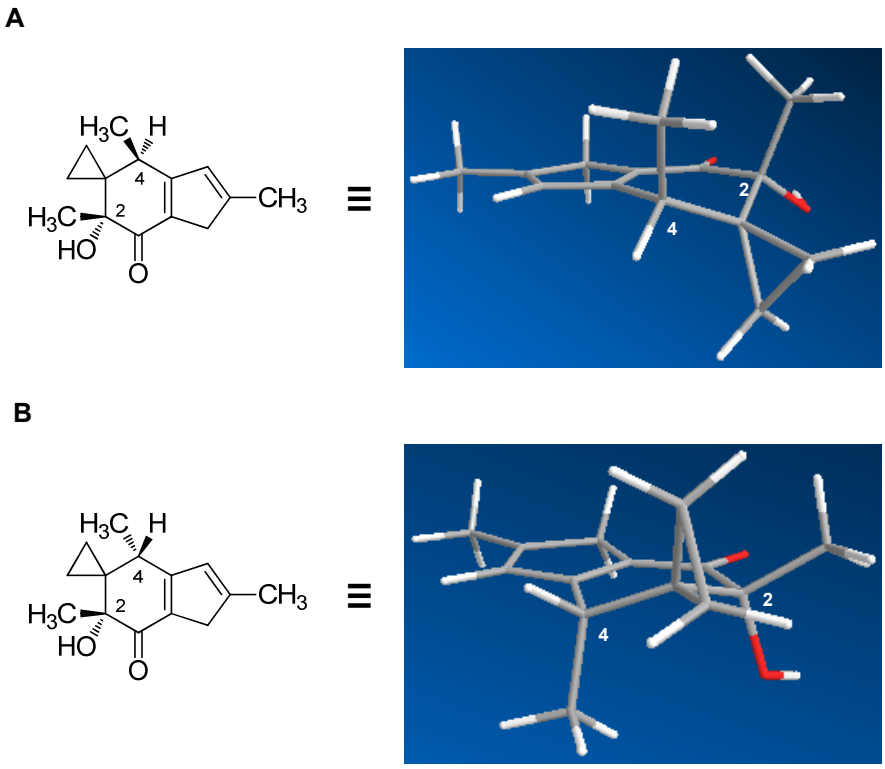

Figure 18. 3-D models of *iso*-M0. A) Hypothetical product of AF reduction with hydride addition to *re* face; B) Actual product of AF reduction with hydride addition to *si* face.

unfavorable 1,3-diaxial steric interactions with each other (Figure 18A). Instead, delivery of the hydride to the *si* face (*syn* to C2-CH_3) occurs, leading to a product with *anti* C2 and C4 methyls, thereby minimizing steric interactions amongst the neighboring alkyl groups (Figure 18B).

The cytotoxicity of *iso*-M0 was tested by Dr. Xiang Yu at the National Institutes of Health in HEK-293T cells transiently transfected to overexpress AOR, together with control cells transfected with a blank vector. Cytotoxicity assays were carried out to test the hypothesis that *iso*-M0 does not require enzymatic reduction to be cytotoxic. Transient transfections do not always occur with consistent efficiency, thereby resulting in varying levels of overexpression in the case of cells transfected with the AOR vector, and cells will lose the ability to overexpress the enzyme over time. Consequently, control compounds must be run for every transfection and results can only be compared relatively. Resulting IC_{50} values confirm the hypothesis the *iso*-M0 is a reactive

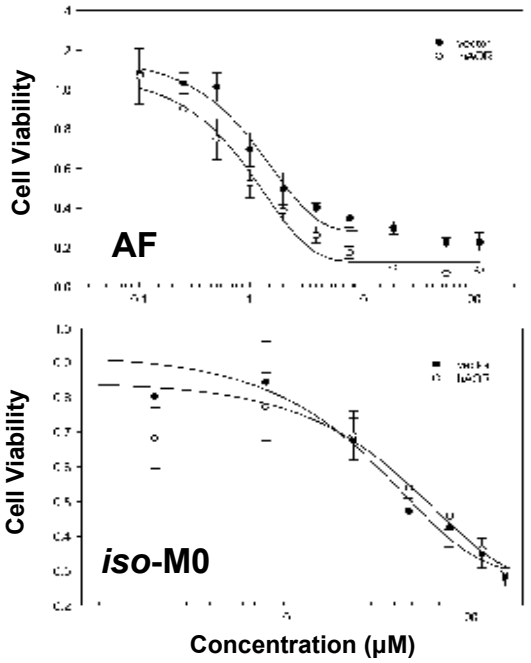

	IC_{50} (μM)*	
	Control	hAOR
AF†	8.1 ± 4.6	2.2 ± 0.5
iso-M0‡	60.6 ± 14.7	71.9 ± 8.1

Figure 19. IC_{50} values for AF and iso-M0 in HEK-293T cells transfected with a blank or hAOR overexpressing vector. Values expressed as Mean ± SE. †n = 5, P = 0.10; ‡n = 3, P = 0.27.

compound that is not influenced by the expression level of AOR. Since *iso*-M0 does not require enzymatic bioactivation, cells are equally sensitive to the compound regardless of enzyme levels, as evidenced by IC_{50} values that are not statistically different for control versus AOR-overexpressing cells (Figure 19). The results suggest that *iso*-M0 reacts like bioactivated AF in cells, i.e. it does not require further activation via enzymatic reduction.

To accurately model a chemically activated form of AF, *iso*-M0 should be capable of reaching nuclear DNA just as bioactivated AF does. This could be tested using the same nuclear extract method as Gong et. al.[10] In addition, one would expect that a positive correlation between cytosolic levels of AOR and AF-DNA adducts, as seen for cells treated with AF[10], would not be present for cells treated with *iso*-M0.

Illudin S or AF can be converted to an aromatic product in the presence of zinc

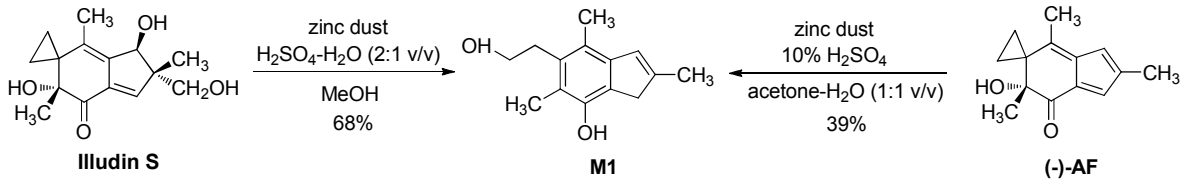

Figure 20. Conversion of illudin S and AF to M1.

and dilute acid,[24] (Figure 20). It was therefore anticipated that *iso*-M0 would decompose to M1 directly, without zinc, in the presence of acid. A consistent chemical mechanism therefore involves tautomerization to M0-enol followed by hydrolytic cyclopropane cleavage (Figure 21). This reactivity profile suggests that *iso*-M0 is a valid chemical model for enzymatically reduced AF. *d-iso*-M0 also undergoes conversion to M1, which further supports the putative reaction mechanism illustrated in Figure 21.

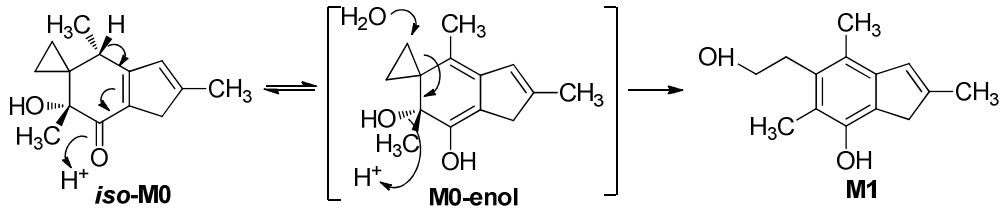

Figure 21. Proposed mechanism for the formation of M1 from *iso*-M0.

In comparing the conditions of the acidic reactions, it was determined that the ratio of THF-d_8:H_2SO_4 was crucial factor in determining the time course of the reaction, i.e. the acidic reaction with a ratio of 2.2 took 30 days to convert to M1, whereas a ratio of 0.5 resulted in overnight conversion of *iso*-M0 to M1. In subsequent NMR timecourse studies, we observed that *iso*-M0 decomposes to M1 at pH 1 with a $t_{1/2}$ of 11.6 h. This was calculated based on the change in integral area for methyl peaks in *iso*-M0 and M1, standardized to the known concentration of the internal standard, dimethyl sulfone. The lack of peaks appearing and disappearing during the extent of the experiment suggests that the proposed intermediates (Figure 21) are so reactive and they cannot be detected

under employed conditions. Further optimization will be required to determine the $t_{1/2}$ at basic and neutral conditions via NMR.

Using a qualitative HPLC-MS/MS method, AF-DNA adducts arising from reactions between *iso*-M0 and dAdo, dGuo, and ctDNA were detected. Comparison of these results with positive controls, where AF in the presence of AOR and NADPH was allowed to react with the same nucleic acid substrates, indicates that *iso*-M0 alkylates DNA with similar relative reactivity profiles (Figure 22). It is evident that the major adduct arising from covalent modification of ctDNA by *iso*-M0 is 3-AF-Ade, which is also the major adduct formed by bioactivated AF. It appears that the deoxyguanosine adduct formed by AF in the presence of AOR and NADPH is also formed by *iso*-M0, but at lower levels.

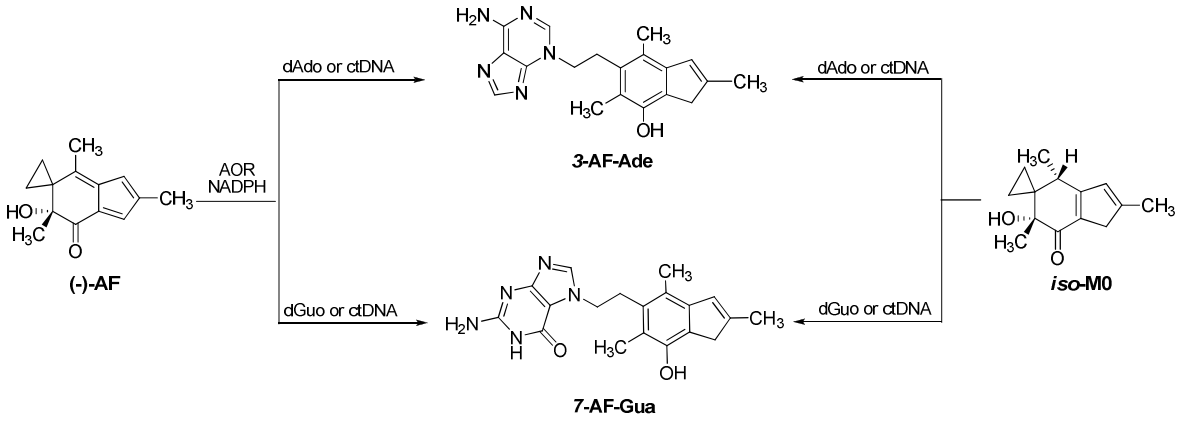

Figure 22. DNA adducts formed from bioactivated AF and iso-M0.

In general, *iso*-M0 seems to alkylate nucleic acids less efficiently than bioactivated AF. For reactions with monomeric nucleosides, 7-AF-Gua and 3-AF-Ade adducts arising from *iso*-M0 were 411- and 29-fold less abundant, respectively, than adducts resulting from covalent modification by bioactivated AF. Adducts formed in ctDNA from *iso*-M0 were less abundant than those resulting from bioactivated AF, but were similar in scale (712- and 750-fold less for 7-AF-Gua and 3-AF-Ade, respectively). Based on observations in the cytotoxicity studies, the lower levels of adduct formation may be attributed to iso-M0's activated status. The outcomes of reactions with ctDNA are different than those with individual nucleosides, especially when analyzing for 3-AF-

Ade adducts in ctDNA reactions as evidenced by one peak per chromatogram (Figure 16A). A previous study of AF-DNA adducts speculates that noncovalent interactions between the compound and duplex DNA may play a role in the observed difference in the alkylation efficiency of AF (by direct alkylation) and bioactivated AF.[10] The compounds under investigation are nearly planar, similar to nucleobases, and one can envision that they are capable of associating with, and perhaps stacking within, the duplex in a non-covalent fashion prior to alkylation, an idea familiar to other alkylators like aflatoxin-B_1,[25] CC-1065, and the duocarmycins.[1] Based the aforementioned examples and our results, we also propose that the structure of duplex DNA increases the likelihood that activated AFs will covalently modify DNA bases, compared to the chance of random interactions between activated AFs and individual nucleosides in solution. This idea is supported by the similar magnitude of difference in adducts formed from *iso*-M0 and bioactivated AF.

It will be of interest to use the quantitative HPLC-MS/MS method developed in our lab[14] to measure number of DNA adducts formed by *iso*-M0 compared to bioactivated AF. Additional future studies will involve measuring the $t_{1/2}$ of AF-DNA adducts in vivo, the persistence of abasic sites that form as a result of adduct depurination, and rates of DNA repair. Assessment of these factors, especially taken together, should allow us to develop a better understanding of how they contribute to AF cytotoxicity.

CONCLUSION

The bio- and chemical activation pathways of AF with AOR and $NaBH_4$, respectively, result in isomeric reactive intermediates that yield the same metabolite M1 and DNA adducts (Figure 23). A new AF derivative that is chemically activated has been obtained and cytotoxicity data suggests that *iso*-M0 does not require further activation to be cytotoxic in cells. Thus, *iso*-M0 appears to be a suitable model of bioactivated AF and is expected to be a useful chemical probe for may be used in future studies investigating covalent interactions with DNA and protein independent of bioactivation.

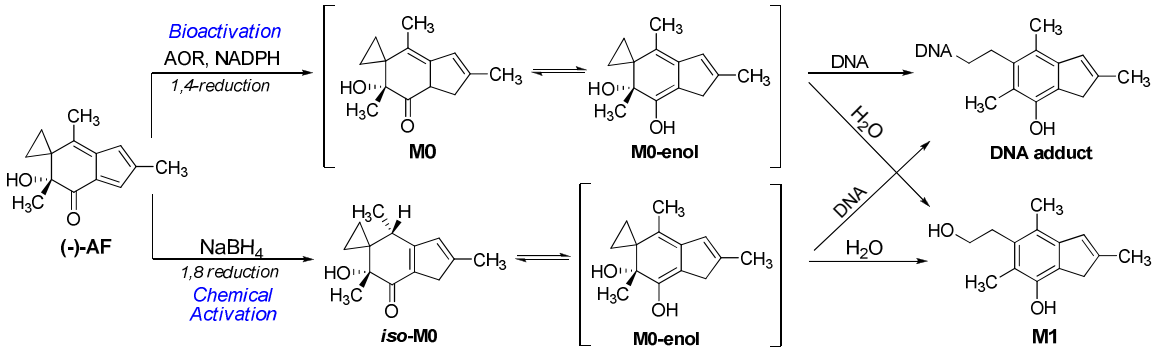

Figure 23. Bioactivated and chemically activated AF yields same metabolite M1 and DNA adducts.

EXPERIMENTAL DETAILS

Chemicals and Enzymes. Illudin S was a gift from MGI Pharma (Bloomington, MN). rAOR was provided by Dr. Thomas Kensler (Johns Hopkins University, Baltimore, MA). $CDCl_3$, D_2O (99.9% D), NaOD (99.5% D, 40% in D_2O), and $NaBD_4$ (90-95% purity) were purchased from Cambridge Isotope Labs, Inc. (Andover, MA). THF-d_8 (99.5% D) was purchased from Sigma-Aldrich (St. Louis, MO). NADPH was purchased from Calbiochem (San Diego, CA). Dimethyl sulfone (Geel, Belgium) was dried under reduced pressure while heating (60 ^oC) for 24 h. Pyridine was dried with an MBraun (Stratham, NH) solvent purification system prior to use. Silica gel (40-63 μm, 60 Å pores) was purchased from Silicycle (Quebec, Canada). All solvents were HPLC grade. AOR and NADPH activity were assessed by monitoring NADPH consumption at A_{340} in the presence of 50 mM *trans*-2-nonenal in 0.5X PBS. dAdo and dGuo hydrate were purchased from MP Biomedicals (Solon, OH) and Tokyo Chemical Industry (Tokyo, Japan), respectively. ctDNA was purchased from Sigma (St. Louis, MO) and ctDNA concentration was determined by measuring absorbance at 260 nm. Reported yields are for an average of two or more experiments and are for material of >95% purity.

Instrumentation and Apparatus. 1-D ^1H and ^{13}C NMR analysis was performed on a 400, 500, or 600 MHz Varian NMR spectrometer, and chemical shifts were assigned on the basis of residual solvent signals. 2-D NOESY spectra were acquired on a 600 MHz Varian NMR spectrometer. Qualitative HPLC-ESI-MS/MS analyses were carried out on an Agilent 1100 capillary flow HPLC interfaced with a Thermo Finnigan LCQ Deca ion trap. HRMS were recorded on a Bruker BioTOF II mass spectrometer with an ESI source using polypropethylene glycol (PPG) as a matrix. UV absorbances were determined with a Varian Cary UV 100 Bio UV-visible spectrophotometer. Xcalibur software was used for the acquisition and processing of MS data.

Qualitative HPLC-ESI-MS/MS analyses were carried out on an Agilent 1100 capillary flow HPLC with a Phenomenex MAX-RP Synergi column (150 x 0.5 mm, 4 μm particle size), interfaced with a Thermo Finnigan LCQ Deca ion trap. The HPLC flow

rate was 10 μL/min and the mobile phase was methanol/0.1% formic acid in H_2O. The mobile phase gradient elution is as follows: 5% methanol in 0.1% formic acid in H_2O to 95% methanol over 19 minutes, then 95% methanol for 11 minutes, returning to initial conditions over 2 minutes, and re-equilibration for 15 minutes. The ESI source was set in positive ion mode with the following parameters: capillary temperature, 250 ^oC; voltage, 3 kV; current, 80 μA; isolation width, 1.5 *m/z*; normalization collision energy, 40%; activation Q, 0.250; activation time, 30 msec. Mass transitions monitored for 3-AF-Ade and 7-AF-Gua adducts were *m/z* 336 to 201 and *m/z* 352 to 201, respectively.

(-)-Acylfulvene. The title compound was synthesized from illudin S as by the following procedure, involving minor modification to the published procedure.[6] Illudin S (205 mg, 0.78 mmol) was dissolved in 70 mL H_2O, followed by the addition of 4N aqueous H_2SO_4 (24 mL, 96 mmol). The reaction stirred at 25 ^oC for 21 h and the solution changed from colorless to yellow and an orange precipitate formed. Ethyl acetate (40 mL) was added to dissolve the precipitate. The aqueous layer was separated and extracted with ethyl acetate (2 x 20 mL). The combined organic layers were washed with saturated sodium bicarbonate (2 x 30 mL), then with brine, dried with magnesium sulfate (anhydrous), filtered, and concentrated by rotary evaporation. The crude product was purified by flash chromatography (90% hexanes/ethyl acetate). Acylfulvene was isolated as a yellow-orange solid (40% yield). ^1H NMR matched published data.[6]

(4'*S*,6'*R*)-6'-hydroxy-2',4',6'-trimethyl-4',6'-dihydrospiro[cyclopropane-1,5'-inden]-7'(1'H)-one (*iso*-M0). A suspension of sodium borohydride (16 mg, 0.4 mmol) in 10 mL pyridine was stirred at 0 ^oC for 10 min under an atmosphere of nitrogen. A solution of (-)-AF (20 mg, 0.09 mmol) in 2 mL pyridine was added dropwise to the $NaBH_4$ suspension over the course of two minutes. The mixture turned from yellow to brown while being allowed to stir at 25 ^oC for exactly 19 min. The reaction was quenched by addition of 3 mL 10% (w/v) aqueous potassium iodate. The resulting mixture was partitioned between water and ethyl acetate, followed by extraction with ethyl acetate (2 x 30 mL). The combined organic layers were washed with brine, dried

with magnesium sulfate (anhydrous), and concentrated by rotary evaporation. The crude product was purified by flash chromatography with elution by a gradient (100% hexanes → 90% hexanes/ethyl acetate). Pentanes were sometimes substituted for hexanes for purification with no change in results. The title compound was isolated as a pale brown oil (43% yield). Caution: *iso*-M0 sublimates under high vacuum. The reported yield is obtained if the sample is under vacuum (2 x 10^{-1} torr) for 3-5 h. NMR spectra are similar to those reported by Neels.[16] ^{1}H NMR (600 MHz, $CDCl_3$) δ 0.33-0.36 (m, 1H), 0.42-0.45 (m, 1H), 0.67-0.71 (m, 2H), 0.95 (d, 3H, *J* = 4.5), 1.40 (s, 3H), 2.17 (s, 3H), 3.13-3.36 (m, 3H), 3.67 (br, 1H), 6.28 (s, 1H). ^{13}C NMR (600 MHz, $CDCl_3$) δ 197.0, 170.0, 157.2, 132.5, 128.5, 74.4, 42.3, 32.9, 30.9, 24.6, 17.3, 12.8, 3.3, 2.1. HRMS *m/z* 241.1185 ($[M+Na]^+$), calcd for $C_{14}H_{18}O_2Na$ 241.1207.

(4'*S*,6'*R*)-4'-deutero-6'-hydroxy-2',4',6'-trimethyl-4',6'-dihydrospiro[cyclopropane-1,5'-inden]-7'(1'H)-one (*d-iso*-M0). The title compound was prepared and purified by the same procedure as iso-M0 detailed above, but with $NaBD_4$ to obtain the product as a pale brown oil (40% yield). ^{1}H NMR (600 MHz, $CDCl_3$) δ 0.33-0.35 (m, 1H), δ 0.42-0.45 (m, 1H), δ 0.68-0.71 (m, 2H), δ 0.94 (s, 3H), δ 1.39 (s, 3H), δ 2.17 (s, 3H), δ 3.13-3.36 (m, 2H), δ 3.66 (br, 1H), δ 6.28 (s, 1H). ^{13}C NMR (600 MHz, $CDCl_3$) δ 197.0, 170.0, 157.2, 132.7, 128.5, 74.4, 42.4, 30.9, 29.9, 24.6, 17.3, 12.7, 3.3, 2.1. HRMS *m/z* 242.1282 ($[M+Na]^+$), calcd for $C_{14}H_{17}DO_2Na$ 242.1267.

Conversion of *iso*-M0 to M1. H_2SO_4 (1.5 mL, 4N aqueous) was added to a solution of *iso*-M0 (8 mg, 0.04 mmol) in 0.8 mL THF. The reaction was allowed to stir for 24 h. M1 precipitated as a pale yellow solid, and was isolated by filtration using a Bucher funnel and filter paper (13% yield). The ^{1}H NMR matched the published spectra for M1.[26]

Conversion of *d-iso*-M0 to M1. H_2SO_4 (1 mL, 5% wt aq) was added to a solution of *d-iso*-M0 (5 mg, 0.002 mmol) in 0.5 mL THF. The mixture was allowed to stir for 19 h. M1 precipitated as a pale yellow solid and was isolated by filtration using a

Bucher funnel and filter paper (10% yield). The ^{1}H NMR matched the published spectra for M1.[26]

Conversion of AF to M1. AF (15 mg, 0.069 mmol) was dissolved in 6 mL acetone-H_2O (1:1 v/v). Zinc dust (160 mg, 2.5 mmol) and 0.75 mL 10% aq. H_2SO_4 was added at 25 ^oC. The reaction mixture turned from yellow to colorless over 1 h. The solution pH was adjusted to pH 8-9 by adding 10% K_2CO_3 (~2 mL, monitored with pH paper), followed by extraction with ethyl acetate (2 x 10 mL). The combined organic layers were washed with brine, dried with magnesium sulfate (anhydrous), and concentrated by rotary evaporation. The crude product was purified by flash chromatography, with gradient elution (10% → 30% ethyl acetate/hexanes) (39% yield). The ^{1}H NMR matched the published spectra for M1.[26]

Nucleic acid reactions with AF, *iso*-M0. In a microcentrifuge tube (1.5 mL) a mixture of test compound (20 µL, 100 mM) and nucleoside were combined and diluted to a final volume of 620 µL with H_2O. The resulting solution was heated at 37 ^oC in a waterbath. *Iso*-M0 reactions and AF negative controls were incubated for 24 h, vortex mixed, and dried by rotary evaporation to remove H_2O.

For bioactivated AF reactions, a mixture of AF (20 µL, 100 mM), nucleoside, AOR (4.2 µL, 1.7 mg/mL), and NADPH (100 µL, 1.5 mM) were combined and diluted to a final volume of 624.2 µL with H_2O. The reactions were incubated in a 37 ^oC waterbath, and additional aliquots of NADPH (100 µL, 1.5 mM) were added at t = 4 h and 24 h. At t = 24 h, an additional aliquot of AOR (4.2 µL, 1.7 mg/mL) was added to the samples. These reactions were incubated for a total of 26.5 h, vortex mixed, heated at 90 ^oC for 1 h, and dried by rotary evaporation to remove H_2O.

Dried samples were extracted with MeOH (3 x 300 µL per sample). Combined extracts were filtered through a 0.45 µm syringe filter and the filter was rinsed with 150 µL MeOH. Filtered extracts were dried by rotary evaporation, transferred to vial inserts with MeOH, and dried again via rotary evaporation. Samples were reconstituted in 16 µL MeOH and analyzed by qualitative HPLC-ESI-MS/MS as described above.

Plasmid construction. Human AOR was PCR-cloned from a human liver cDNA library (Clontech, Mountain View, CA) according to the NCBI GenBank sequence using the following primer set:

Forward: 5'-GTCGCGGAATTCAGCTTCAGGATGGTTCGTACTAAGACATGG

Reverse: 5'-GTCGCGCTCGAGTTACTATCATGCTTTCACTATTGTCTTCCCC.

PCR product was cleaned and ligated into pBlueScript between *Eco*RI and *Xho*I sites. DNA insert was confirmed by sequencing and subcloned into episomal vector pCEP4.

Cell Culture and Transfection. 293T cells were obtained from the American Type Culture Collection (ATCC, Manassas, VA) and maintained in Dulbecco's Modified Eagle's Medium (high glucose, Invitrogen, Inc., Carlsbad, CA) with 10% heat-inactivated fetal bovine serum. Cells were incubated at 37°C in a humidified atmosphere containing 5% CO_2. Cells were transiently transfected with Lipofectamine 2000 reagents (Invitrogen, Inc.).

Cell Viability Assay. pCEP4 and pCEP4-hAOR transfected 293T cells were maintained in DMEM supplemented with fetal bovine serum and seeded 24 hour prior in 96-well plates at a density of 4000 cells/well. Treatments were initiated by replacing the media with those containing AF or *iso*-M0 at indicated concentrations (cisplatin used as a positive control). Cell viability was measured 24 hr later via CellTiter-Blue assay, which measures the metabolic capacity of viable cells to reduce the dye resazurin, to a fluorescent compound (Promega Corporation, Madison, WI). Linear regression analysis and IC_{50} calculations were performed using SigmaPlot (Version 11.0).

Kinetic study of *iso*-M0 to M1. H_2SO_4 (1 mL, 4N) was added to an NMR tube containing a solution of *iso*-M0 (6.76 mg) and dimethyl sulfone (6.4 mg) in THF-d_8 (0.5 mL) in an NMR tube. The ensuing reaction was monitored by NMR (600 MHz, Varian) using a pre-acquisition delay experiment, taking 4 scans every 5 minutes for 12 hours.

Integrals were measured manually and normalized to the integral of the internal standard. Plots were generated using KaleidaGraph (version 4.0).

REFERENCES

1. Boger, D.L. and R.M. Garbaccio, *Shape-Dependent Catalysis: Insights into the Source of Catalysis for the CC-1065 and Duocarmycin DNA Alkylation Reaction.* Accounts of Chemical Research, 1999. **32**(12): p. 1043-1052.
2. Lin, A.J., et al., *Potential bioreductive alkylating agents. 1. Benzoquinone derivatives.* Journal of Medicinal Chemistry, 1972. **15**(12): p. 1247-1252.
3. Moore, H.W., *Bioactivation as a Model for Drug Design Bioreductive Alkylation.* Science, 1977. **197**: p. 527-32.
4. Chen, Y., Hu, L., *Design of Anticancer Prodrugs for Reductive Activation.* Medicinal Research Reviews, 2009. **29**: p. 29-64.
5. Gates, K.S., *An Overview of Chemical Processes That Damage Cellular DNA: Spontaneous Hydrolysis, Alkylation, and Reactions with Radicals.* Chemical Research in Toxicology, 2009. **22**(11): p. 1747-1760.
6. McMorris, T.C., et al., *Acylfulvenes, a new class of potent antitumor agents.* Experientia, 1996. **52**(1): p. 75-80.
7. Kelner, M.J., et al., *Preclinical evaluation of illudins as anticancer agents.* Cancer Res, 1987. **47**(12): p. 3186-9.
8. McMorris, T.C., et al., *(Hydroxymethyl)acylfulvene: an illudin derivative with superior antitumor properties.* J Nat Prod, 1996. **59**(9): p. 896-9.
9. McMorris, T.C., et al., *Structure and reactivity of illudins.* Tetrahedron, 1989. **45**(17): p. 5433-5440.
10. Gong, J., et al., *Depurinating acylfulvene-DNA adducts: characterizing cellular chemical reactions of a selective antitumor agent.* J Am Chem Soc, 2007. **129**(7): p. 2101-11.
11. Dick, R.A., X. Yu, and T.W. Kensler, *NADPH alkenal/one oxidoreductase activity determines sensitivity of cancer cells to the chemotherapeutic alkylating agent irofulven.* Clin Cancer Res, 2004. **10**(4): p. 1492-9.
12. Gong, J., et al., *Investigating the role of stereochemistry in the activity of anticancer acylfulvenes: synthesis, reductase-mediated bioactivation, and cellular toxicity.* J Med Chem, 2006. **49**(8): p. 2593-9.
13. Dick, R.A., et al., *Antioxidative function and substrate specificity of NAD(P)H-dependent alkenal/one oxidoreductase. A new role for leukotriene B4 12-hydroxydehydrogenase/15-oxoprostaglandin 13-reductase.* J Biol Chem, 2001. **276**(44): p. 40803-10.
14. Neels, J.F., et al., *Quantitative correlation of drug bioactivation and deoxyadenosine alkylation by acylfulvene.* Chem Res Toxicol, 2007. **20**(10): p. 1513-9.
15. Dick, R.A. and T.W. Kensler, *The catalytic and kinetic mechanisms of NADPH-dependent alkenal/one oxidoreductase.* J Biol Chem, 2004. **279**(17): p. 17269-77.
16. Neels, J.F., *Antitumor Acylfulvenes: Chemical and Biological Reactivity*. 2007, University of Minnesota: Minneapolis, MN.

17. Jackson, W.R. and A. Zurqiyah, *The occurrence of 1,2- or 1,4-addition in the reduction*
of some α,β - unsaturated ketones with metal hydrides. Journal of the Chemical Society, 1965: p. 5280-5287.
18. Gong, J., Sturla, S. J., *Unpublished results.*
19. Hays, P.A., *Proton Nuclear Magnetic Resonance Spectroscopy (NMR) Methods for Determining the Purity of Reference Drug Standards and Illicit Forensic Drug Seizures.* J Forensic Sci, 2005. **50**(6): p. 1342.
20. Erker, G., et al., *Cp-substituent additivity effects controlling the stereochemistry of the propene polymerization reaction at conformationally unrestricted (Cp-CHR1R2)2ZrCl2/methylalumoxane catalysts.* Journal of the American Chemical Society, 1991. **113**(20): p. 7594-7602.
21. Sweeney, N.J., et al., *Novel benzyl substituted titanocene anti-cancer drugs.* Journal of Organometallic Chemistry, 2005. **690**(21-22): p. 4537-4544.
22. McMorris, T.C., *Discovery and development of sesquiterpenoid derived hydroxymethylacylfulvene: a new anticancer drug.* Bioorg Med Chem, 1999. **7**(5): p. 881-6.
23. Carey, F.A. and R.J. Sundberg, *Advanced Organic Chemistry, Part B: Reactions and Synthesis*. Fifth ed. 2007: Springer.
24. McMorris, T.C. and M. Anchel, *Fungal Metabolites. The Structures of the Novel Sesquiterpenoids Illudin-S and -M.* J Am Chem Soc, 1965. **87**: p. 1594-600.
25. Smela, M.E., et al., *The chemistry and biology of aflatoxin B1: from mutational spectrometry to carcinogenesis.* Carcinogenesis, 2001. **22**(4): p. 535-545.
26. McMorris, T.C., et al., *Metabolism of antitumor acylfulvene by rat liver cytosol.* Biochem Pharmacol, 1999. **57**(1): p. 83-8.